Direct tensile behavior and size effect of strain-hardening fiber-reinforced cement-based composites (SHCC)

K. Rokugo & Y. Uchida
Department of Civil Engineering, Gifu University, Japan

M. Moriyama
Central Nippon Expressway Co., Ltd., Japan

S.-C. Lim
Deros Co., Ltd, Japan

ABSTRACT: A simple tension test method on dumbbell specimens for strain-hardening fiber-reinforced cement-based composites (SHCC) was proposed. Tension tests were reliably accomplished using the test apparatus proposed in this study, with all specimens broken in their test zones. Though the tensile strength and the tensile yield strength scarcely varied between the specimen thicknesses, the ultimate tensile strain scattered more widely as the specimen thickness increased. Regardless of the thickness, the crack widths of all specimens increased up to a strain of approximately 1%. When the strain exceeded 1%, the crack width of specimens with an ultimate tensile strain of 4% or more scarcely increased as the strain increased, with the maximum crack width being not more than 0.2 mm.

1 INTRODUCTION

Technology in the concrete engineering field is for the most part intended to control cracking in concrete, to the extent that "concrete engineering" could be renamed as "crack control engineering." Crack width can be controlled to a certain extent by making the structure reinforced with steel, and cracking can be prevented by employing prestressed concrete technique. Various measures are also taken for materials and placing to suppress hydration heat and inhibit shrinkage, which causes cracking in concrete.

Conventionally, the purpose of including short fibers in concrete has been primarily to increase its tensile strength, as in steel fiber-reinforced concrete. Fibers added for the purpose of controlling the crack width have recently attracting attention. A composite material referred to as High Performance Fiber-Reinforced Cement Composite (HPFRCC) has been developed. This material is called Strain-Hardening fiber-reinforced Cement-based Composites (SHCC).

This material allows substantial tensile deformation as narrow cracks occur one after another under increasing tensile forces. The crack width is controlled by short fibers to a level of 0.1 mm and not more than 0.2 mm. This material is characterized by the increase in the number of cracks, instead of the crack width, associated with the increase in the tensile deformation.

These characteristics that distinguish this material from conventional mortars and concretes should be effectively suited to the purposes and conditions of the intended use. To this end, it is vital to elucidate the ultimate tensile strain (peak tensile strain), tensile stress-strain curve, cracking performance (width, number, and spacing), and size effect on these tensile performances, as well as to establish test methods for evaluating these tensile performances(Li 1993, Li 2002, Kunieda & Rokugo 2006).

This study aims to propose a simple tension test method on dumbbell specimens for SHCC showing strain-hardening behavior. Uniaxial direct tension tests were also conducted using the proposed method to investigate the tensile performance of SHCC and the effect of specimen thickness on such performance.

2 PROPOSAL FOR A UNIAXIAL TENSION TEST METHOD AND TEST APPARATUS

2.1 *Performance required for tension test methods and problems*

The key tensile performance items for evaluating SHCC include the following: crack width, number of cracks, crack spacing, tensile strength, tensile yield strength, and ultimate tensile strength. For stable measurement of these items by tension testing, measures should be taken for the following three points: (1) to transfer the tensile forces from the testing machine to the specimen without causing failure of the enlarged ends; (2) to suppress the L-shaped (non-uniform) deformation of the specimen; and (3) to stably control the behavior in the strain-hardening region after the first crack. In regard to point (2) above, L-shaped deformation is essentially unavoid-

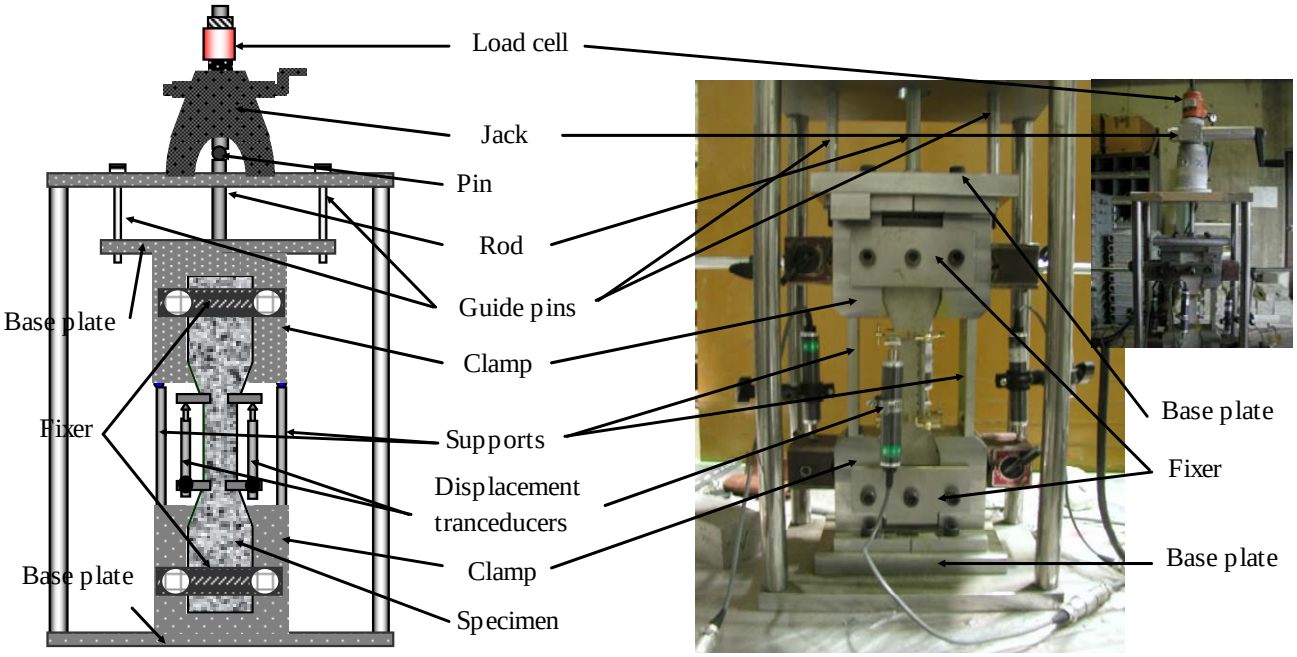

Figure 1. Tension test apparatus.

able, as a crack will develop from a point of a specimen to the entire cross-section, but could be reduced to a certain extent. It should be noted that L-shaped deformation of SHCC is not as large as that of normal concrete, as each crack width of SHCC tends to remain small while the crack develops.

In this study, a simple tension testing machine was developed with the aim of solving the above-mentioned problems of tension testing and permitting easy observation of multiple cracks occurring in the specimen, with due consideration given to the operability and safety.

2.2 *Tension test apparatus and operation*

The tension test apparatus developed in this study is shown in Fig. 1. The shoulders of a dumbbell specimen are engaged in the upper and lower locks in the steel framing with a mass of approximately 30 kg and external size of 250 by 200 by 500 mm. Though frictional clamping of specimens is generally employed, shoulder locking was adopted in this study to transfer tensile forces to specimens.

To facilitate engaging and disengaging of specimens into and from the apparatus, the clamp on one side of each lock (the left side clamps of the upper and lower locks shown in Fig. 1) is fixed to the base plate. The clamp on the other side of each lock (the right side clamps) is designed to slide sideways with a travel of 5 mm. After engaging a specimen, the clamps on the right side are set in place and bolted to the base plates. Both clamps of the upper and lower locks are fastened together using lock fasteners. Tie rods are employed to align the upper and lower locks.

A mechanical jack is mounted on the steel frame to apply tensile forces to the specimen through a force-applying rod. The upper lock is pulled up by the applied force along the two guide pins. In regard to the boundary conditions of tension testing, the lower lock is fixed to the base plate of the steel frame (fixed support), whereas the upper lock is pin-supported by the force-applying rod via a hinge set in the bar.

The load-displacement relationship during tension testing was measured using displacement transducers directly set on the specimen and a load cell placed on top of the loading element.

3 TENSILE PERFORMANCE AND SIZE EFFECT

3.1 *Experiment overview*

3.1.1 *Materials*

Table 1 gives the mix proportions of SHCC and the physical properties of short fibers. Premixed polymer cement mortar containing 323 kg/m^3 of coarse aggregate with a maximum size of 10 mm was used as the matrix of SHCC. Polyvinyl alcohol (PVA) fibers 12 mm in length and 40 μm in diameter were blended with the matrix at a ratio of 2% by volume. The unit water content was 257 kg/m^3. The slump flow and air content were 420 mm and 6.8%, respectively. All the materials for SHCC were placed in a mixer and mixed for 5 min. When placing SHCC, the molds were tapped with a mallet instead of using a tamping rod or internal vibrator. The specimens were demolded two days after placing and then air-cured in a laboratory with a room temperature of 10 to 20 degrees Celsius until testing at 28 to 36 days. Specimens for compression and bending tests were

Table 1. Mix proportions of SHCC.

Units (kg/m^3)					Slump flow (mm)	Air content (%)
Mortar	Aggregate	Polymer	Water	Fiber		
1225	323	71	257	26.0	420	6.8

Table 2. Compression test results.

Name	Thickness (mm)	Compressive strength (MPa)	Elastic modulus (GPa)
PVA-13	13	34.4	16.3
PVA-30	30		
PVA-50	50		

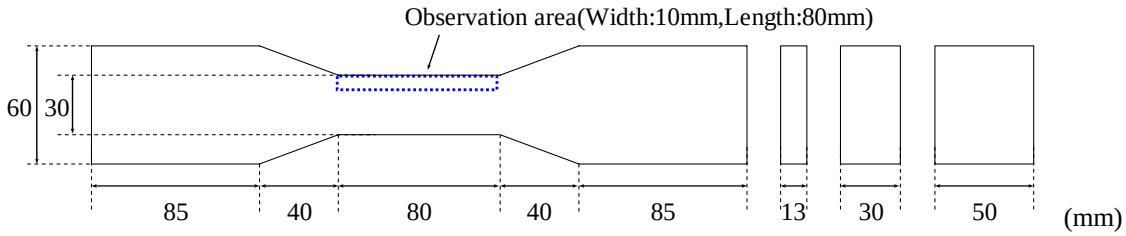

Figure 2. Specimen geometry.

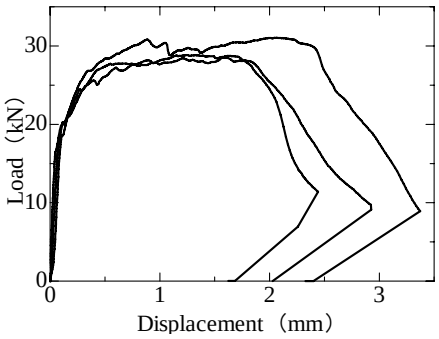

Figure 3. Flexural load-displacement relationship.

also fabricated by the same method as tension test specimens.

3.1.2 *Specimens*

Table 2 and Fig. 2 show the outline of tension specimens and the geometry of dumbbell specimens, respectively. The shape and size of the plan of tension specimens were kept constant, while the thickness was varied in three levels: 13, 30, and 50 mm. Five specimens each were produced for each thickness.

3.1.3 *Tensile loading testing*

Figure. 1 show the outline of crack observation and the state of tensile loading testing, respectively. The displacement of a gage length of 80 mm in the center of each specimen was measured with sensitive displacement transducers with an accuracy of 1/1,000 mm set on both sides. The loading speed was around 0.5 mm/min.

Cracking in three specimens for each size was observed with a microscope (VH-5000 manufactured by Keyence Corporation) while stopping the loading at tensile strain levels of 0.25%, 0.63%, 0.95%, 1.25%, 1.88%, 2.5%, 3.13%, 3.75%, and 5.0%. The observation area was the area 80 mm in length and 10 mm in width on the bottom (molded surface) near the side surface of each specimen where cracking appears to be widest and easy to observe. The microscope with a magnification of 25 was moved along this area to measure the cracks.

3.2 *Compression and bending test results*

Table 2 and Fig. 3 show the compression and bending test results. Bending tests were conducted by third-point loading. The compressive strength and elastic modulus were 34.4 MPa and 16.3 GPa, respectively. The flexural load-displacement relationship clearly shows increases in the load as the displacement (strain) increases after cracking, the so-called “deflection hardening characteristics.” Also, multiple fine cracks were visually observed after bending testing.

3.3 *Tension test results and discussion*

Tension tests were reliably accomplished using the test apparatus proposed in this study, with all specimens being broken in their test zones.

3.3.1 *Size effect on stress-strain relationship*

Figure 4 shows the tensile stress-strain relationship of each thickness of tension specimens. Strain hardening characteristics, in which the tensile stress increases as the strain increases without brittle failure after the first cracking, are observed in specimens of all thicknesses. The ultimate tensile strains widely scatter.

The average tensile strength is approximately 4 MPa with no appreciable difference between thick-

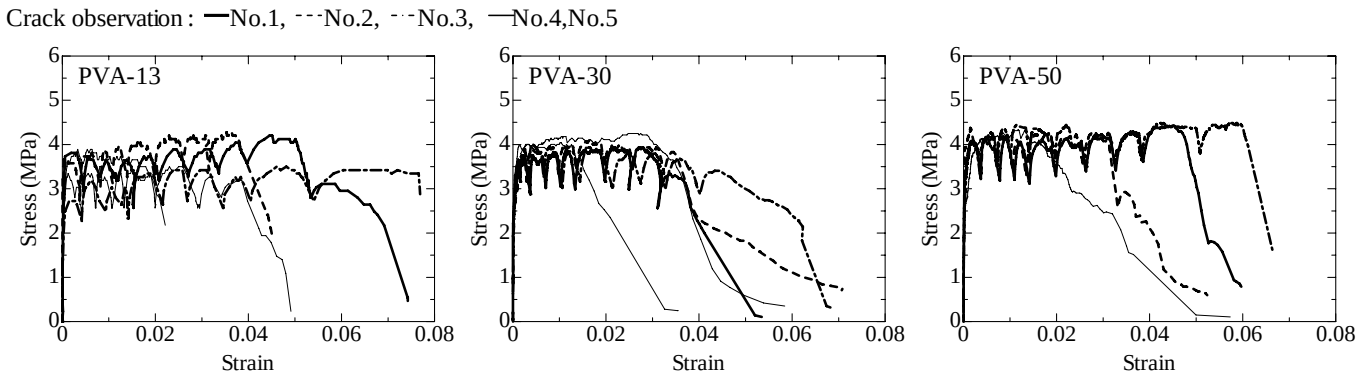

Figure 4. Tensile stress-strain relationship.

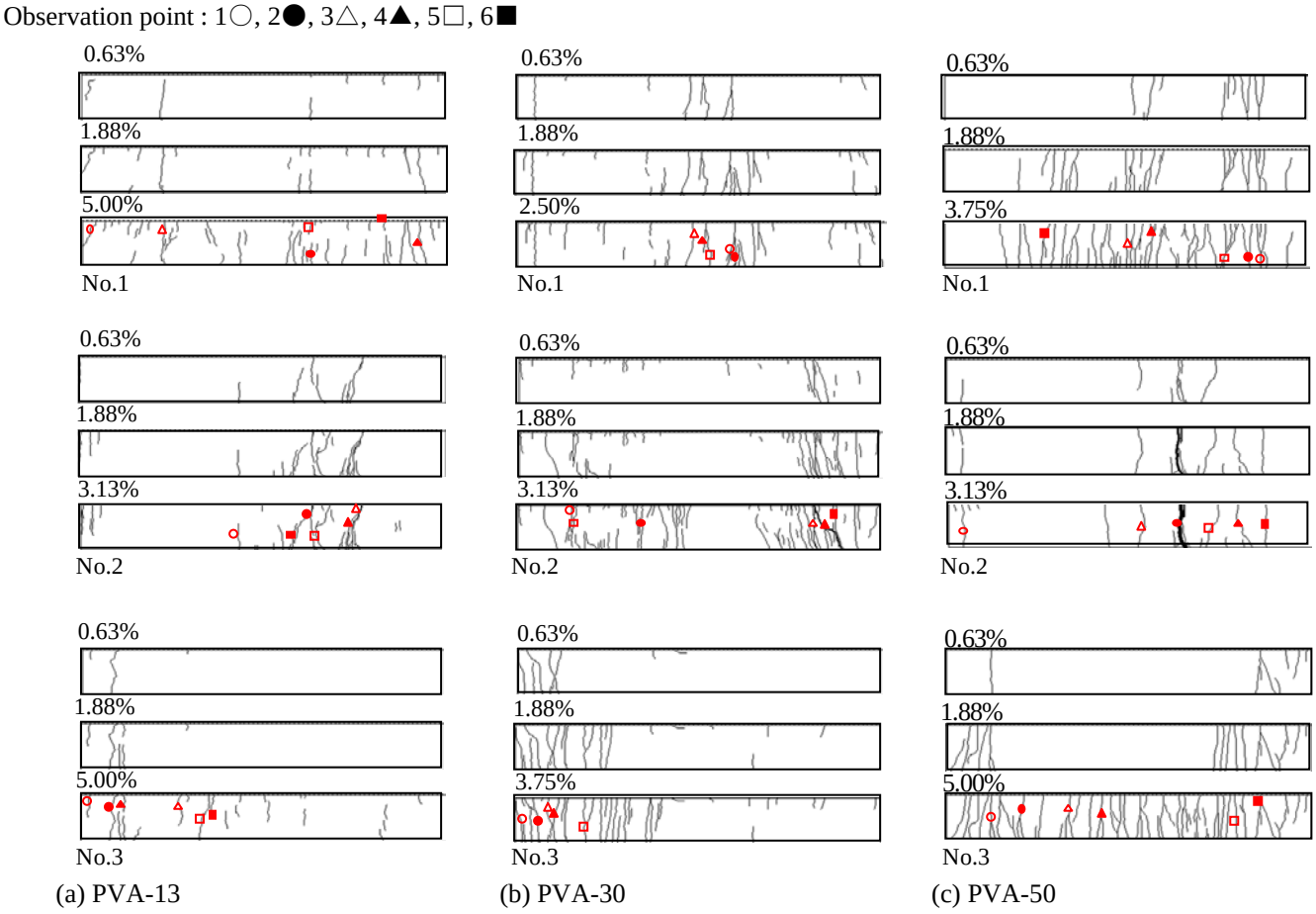

Figure 5. Crack patterns of specimens at tensile strain stages.

nesses. However, the tensile strength of 13 mm-thick specimens widely scatters when compared with other thicknesses.

The tensile yield strength showed no appreciable difference between thicknesses. However, the ultimate tensile strain of 13 mm- and 30 mm-thick specimens concentrates around 3% to 4%, whereas that of 50 mm-thick specimens widely scatters from 2% to 6%.

3.3.2 *Cracking tendencies and size effect*

Figure 5 shows the crack patterns of specimens at tensile strain stages of 0.63% and 1.88%, as well as the final strain stage observed by a microscope. Cracks expressed as bold lines in the figure represent particularly wide cracks.

Multiple cracks are found in all specimens, with their number increasing as the strain increases. A higher ultimate strain leads to a larger number and area of cracks in specimens of all thicknesses.

In the case of specimen No. 3 with a thickness of 13 mm, however, its ultimate tensile strain is 5% or more, but the number of cracks is smaller than other specimens with an ultimate tensile strain of around 3%. This can be attributed to the small area of microscopic crack observation rather than the effect of different thicknesses.

The cracks of 50 mm-thick specimens tend to be long, whereas those of 13 mm-thick specimens tend to be very short, and their numbers and length increase as the strain increases, with new short cracks developing. The crack patterns of 30 mm-thick

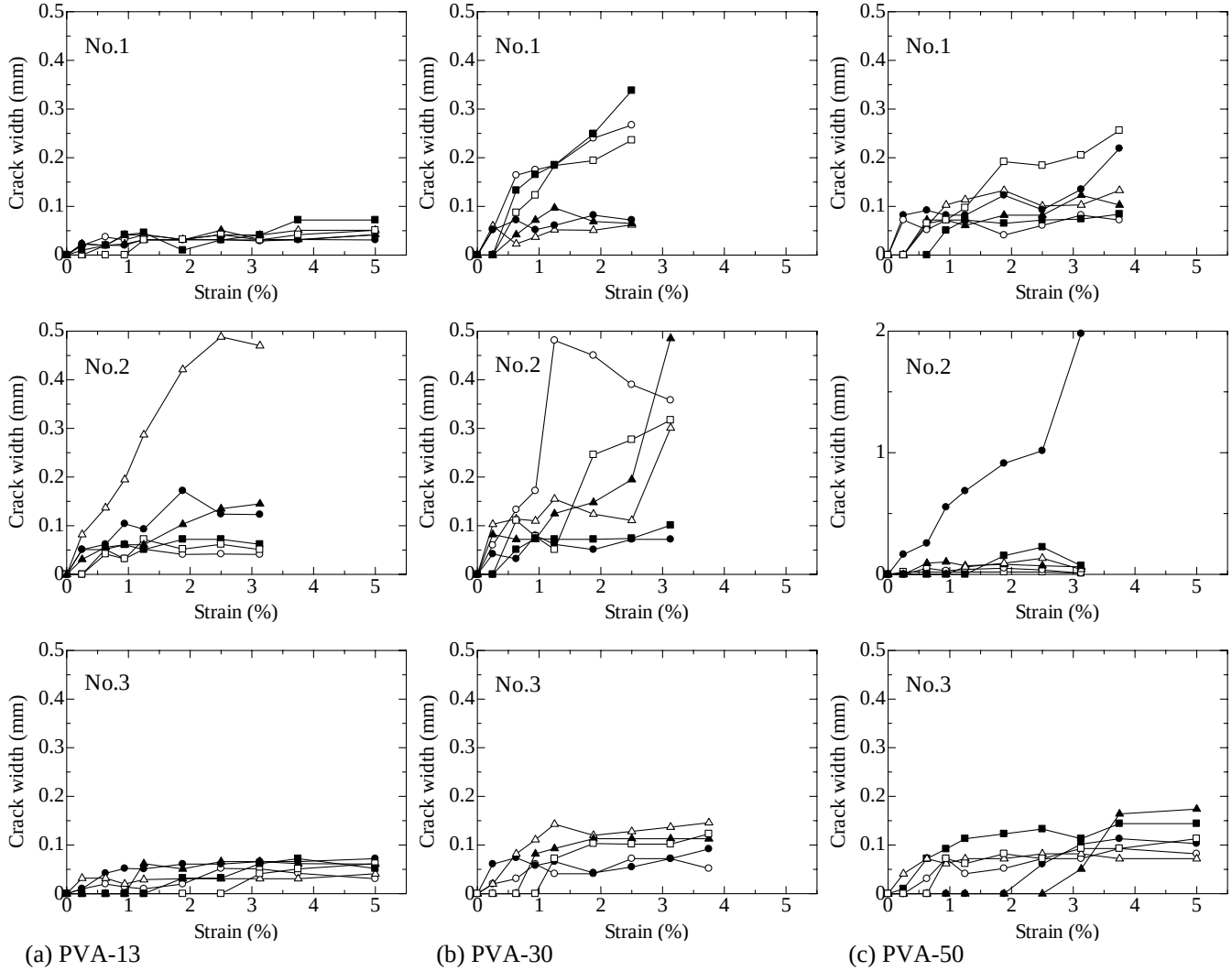

Figure 6. Crack width-strain relationships.

specimens are intermediate between the other two thicknesses.

3.3.3 *Crack width and size effect*

Figure 6 shows the crack width-strain relationships. The widths of the cracks measured using a microscope, which are shown with blocks (1 to 6) in Fig. 5, are shown with the same blocks in Fig. 6. Measurement was made for the first three cracks and the three widest cracks in each specimen. In regard to specimens with an ultimate tensile strain of 4% or more (as indicated in each graph), the crack width increases up to a strain of approximately 1% but the increment of crack width becomes very small, with the maximum crack width being not more than 0.2 mm. However, the maximum crack width tends to scatter more widely as the specimen thickness increases. Nevertheless, this requires further investigation over a wider range of crack observation.

In regard to specimens with an ultimate tensile strain of less than 4% (as indicated in each graph), crack width development is classified into two types with a strain of over 1%: the crack width rapidly increases in one type and scarcely increases in the other type. As inferred from Fig. 5, this is presumably due to relative localization of cracking. This tendency is common to all thicknesses.

4 CONCLUSIONS

The results of direct uniaxial tension tests are summarized as follows:

- Tension tests were reliably accomplished using the test apparatus proposed in this study, with all specimens broken in their test zones.
- Strain hardening characteristics were observed in specimens of all thicknesses. Though the tensile strength and the tensile yield strength scarcely varied between the specimen thicknesses, the ultimate tensile strain scattered more widely as the specimen thickness increased.
- In regard to cracking properties, each crack in 50 mm-thick specimens is long, whereas it is short in 13 mm-thick specimens, and its length increases as the strain increases, while new short cracks begin to appear.

– Regardless of the thickness, the crack widths of all specimens increased up to a strain of approximately 1%. When the strain exceeded 1%, the crack width of specimens with an ultimate tensile strain of 4% or more scarcely increased as the strain increased, with the maximum crack width being not more than 0.2 mm. In specimens with the ultimate tensile strain of less than 4%, however, two increasing patterns in the crack width were observed after the strain exceeded 1%. In one pattern, the crack width significantly increased as the strain increased, whereas it scarcely increased in the other pattern.

REFERENCES

Li, V.C. 1993. From Micromechanics to Structural Engineering -The Design of Cementitious Composites for Civil Engineering Applications. *J. Struct. Mech.Earthquake Eng.*, JSCE, 10 (2): 37-48.

Li. V.C. 2002. Reflections on the Research and Development of Engineered Cementitious Composites (ECC), *Proceedings of the JCI International Workshop on Ductile Fiber Reinforced Cementitious Composites (DFRCC) - Application and Evaluation*, JCI: 1-21.

Kunieda, M. & Rokugo, K. 2006. Recent Progress on HPFRCC in Japan - Required Performance and Applications -, *Journal of Advanced Concrete Technology*, JCI, 4(1): 19-33.